THE JOURNAL OF BIOLOGICAL CHEMISTRY VOL. 290, NO. 19, pp. 12184–12194, May 8, 2015

UV Light Potentiates STING (Stimulator of Interferon Genes)-dependent Innate Immune Signaling through Deregulation of ULK1 (Unc51-like Kinase 1)*

Received for publication, March 2, 2015, and in revised form, March 19, 2015 Published, JBC Papers in Press, March 19, 2015, DOI 10.1074/jbc.M115.649301

Michael G. Kemp[1], **Laura A. Lindsey-Boltz, and Aziz Sancar**[2]

From the Department of Biochemistry and Biophysics, University of North Carolina School of Medicine, Chapel Hill, North Carolina 27599

Background: UV wavelengths of sunlight exacerbate the symptoms of autoimmunity.
Results: UV and UV-mimetic chemical carcinogens stimulate STING-dependent innate immune signaling in keratinocytes and other human cells by disrupting the STING negative regulator ULK1.
Conclusion: STING-dependent innate immune signaling is elevated in UV-irradiated human cells.
Significance: Deregulation of innate immune signaling by UV light may contribute to autoimmunity.

The mechanism by which ultraviolet (UV) wavelengths of sunlight trigger or exacerbate the symptoms of the autoimmune disorder lupus erythematosus is not known but may involve a role for the innate immune system. Here we show that UV radiation potentiates STING (stimulator of interferon genes)-dependent activation of the immune signaling transcription factor interferon regulatory factor 3 (IRF3) in response to cytosolic DNA and cyclic dinucleotides in keratinocytes and other human cells. Furthermore, we find that modulation of this innate immune response also occurs with UV-mimetic chemical carcinogens and in a manner that is independent of DNA repair and several DNA damage and cell stress response signaling pathways. Rather, we find that the stimulation of STING-dependent IRF3 activation by UV is due to apoptotic signaling-dependent disruption of ULK1 (Unc51-like kinase 1), a pro-autophagic protein that negatively regulates STING. Thus, deregulation of ULK1 signaling by UV-induced DNA damage may contribute to the negative effects of sunlight UV exposure in patients with autoimmune disorders.

The symptoms of a number of autoimmune diseases, including systemic lupus erythematosus (SLE),[3] have long been known to be triggered or exacerbated by exposures to ultraviolet (UV) wavelengths of sunlight that damage genomic DNA and other cellular biomolecules (1–3). This damage and associated cell death is thought to result in the release of potential autoantigens, including DNA and other nuclear proteins, which are taken up by macrophages to initiate autoantibody development or targeted by the adaptive immune system.

In addition, DNA from dying cells as well as DNA from viruses and microbial pathogens are known to be strong immune stimulants that can accumulate in the cytosol of infected cells and activate an intracellular signal transduction cascade that produces various immune system modulators and proinflammatory cytokines (4, 5). This pathway is critically dependent on a protein known as STING (stimulator of interferon genes; also known as TMEM173, MITA, MYPS, and ERIS) (6–8), which responds not to DNA directly but to the cyclic dinucleotide 2′,3′-cGAMP that is produced upon the stimulation of the enzyme cGAS (cyclic GMP-AMP synthase) by cytosolic DNA (9–15). The binding of STING to 2′,3′-cGAMP and related cyclic dinucleotides that are produced by microbial pathogens (16–19) causes a conformational change in STING (20, 21) that is thought to allow it to function as a scaffold protein to mediate the phosphorylation and activation of IRF3 (interferon regulatory factor 3) by the upstream kinase TBK1 (TANK-binding kinase 1) (22). This phosphorylation event induces IRF3 homodimerization and is required for IRF3 to function as a transcription factor for a variety of gene targets, including type I interferons, pro-inflammatory cytokines, and pro-apoptotic factors (23–26).

The major model for UV stimulation of immune responses involves the abnormal clearance of DNA or other cellular constituents that are released from dying cells and then taken up by macrophages and other immune cells (27–31). However, there may be additional mechanisms that take place in viable and non-immune cells, such as keratinocytes, that modulate immune signaling within the skin and throughout the body. In

* This work was supported, in whole or in part, by National Institutes of Health Grants R01GM32833 and R21ES024425 (to A. S.) and P30ES010126 (UNC Center for Environmental Health and Susceptibility Pilot Project Award; to M. K.).

[1] To whom correspondence may be addressed: Dept. Biochemistry and Biophysics, Campus Box 7260, University of North Carolina School of Medicine, Chapel Hill, NC 27599. Tel.: 919-966-7489; Fax: 919-966-2852; E-mail: michael_kemp@med.unc.edu.

[2] To whom correspondence may be addressed: Dept. of Biochemistry and Biophysics, Campus Box 7260, University of North Carolina School of Medicine, Chapel Hill, NC 27599. Tel.: 919-962-0115; Fax: 919-966-2852; E-mail: aziz_sancar@med.unc.edu.

[3] The abbreviations used are: SLE, systemic lupus erythematosus; STING, stimulator of interferon genes; cGAMP, cyclic GMP-AMP; cGAS, cyclic GMP-AMP synthase; IRF3, interferon regulatory factor 3; IRF3-P, phospho-IRF3; TBK1, Tank-binding kinase 1; ULK1, Unc51-like kinase 1; BPDE, benzo[a]pyrene-7,8-dihydrodiol-9,10-epoxide; AAF, *N*-acetyoxy-2-acetylaminofluorene; ISD, interferon-stimulatory DNA; ATM, ataxia telangiectasia-mutated; pIC, polyinosinic-polycytidilyic acid; ATR, Ataxia telangiectasia-mutated and Rad3-related; Chk1, checkpoint kinase 1; c-di-GMP, cyclic di-GMP; AMBRA1, autophagy/beclin-1 regulator 1; LKB1, liver kinase B1; AMPK, AMP-activated protein kinase.

this report, we show that UV and UV-mimetic chemical carcinogens stimulate STING-dependent IRF3 activation in response to cytosolic DNA and cyclic dinucleotides in keratinocytes and other human cells. Moreover, we find that this effect is independent of DNA repair and several major UV-dependent DNA damage response and cell stress signaling pathways. Instead, abrogation of the negative STING regulator and pro-autophagic factor ULK1 (Unc51-like kinase 1) (32) by UV-induced apoptotic signaling is responsible for potentiating the cellular innate immune responses to cytosolic DNA and cyclic dinucleotides. These data therefore provide a novel mechanism by which UV and related environmental genotoxins may trigger or exacerbate autoimmunity in susceptible individuals.

EXPERIMENTAL PROCEDURES

Cell Lines—Human THP-1 monocytes, HaCaT keratinocytes, and HEK293T cells were cultured at 37 °C in a 5% CO_2 humidified incubator in either RPMI1640 or Dulbecco's modified Eagle's medium supplemented with 10% fetal bovine serum and penicillin/streptomycin. HEK293T cells stably expressing HA-tagged STING were generated by transfection of pUNO1-hSTING-HA3x (Invivogen) and selection with blasticidin. To expose cells to UV radiation, cells were placed under a GE germicidal lamp that emits primarily 254-nm UV light (UV-C) connected to a digital timer and irradiated with the indicated fluences of UV light (typically 100 J/m^2). Other genotoxic compounds were added directly to tissue culture media as indicated. Fractionation of cells to yield cytosolic and nuclear fractions was performed as previously described (33).

Chemicals and Reagents—The 45-nucleotide-long sense and antisense strands of interferon-stimulatory DNA (ISD) oligonucleotides (23) were synthesized by Sigma, resuspended in 10 mM Tris-HCl, pH 8.0, 1 mM EDTA, 100 mM NaCl, and then annealed by heating to 90 °C for 5 min and slow cooling to room temperature. Benzo[a]pyrene-7,8-dihydrodiol-9,10-epoxide (BPDE) and *N*-acetoxy-2-acetylaminofluorene (AAF) were obtained from the NCI Chemical Carcinogen Reference Standard Repository (Midwest Research Institute, MO). Cycloheximide, the p38 inhibitor SB202190, the Jun kinase (JNK) inhibitor SP600125, the MEK1/2 inhibitor U0126, the ATM (ataxia telangiectasia-mutated) kinase inhibitor KU-55933, the DNA-PK (DNA-dependent protein kinase) inhibitor NU7026, the Chk1 (checkpoint kinase 1) inhibitor PF-477736, lipopolysaccharide, and polyinosinic-polycytidilyic acid (pIC) were purchased from Sigma. The ATR (ataxia-telangiectasia-mutated and Rad3-related) inhibitor VE-821 was purchased from Selleckchem. 2′,3′-cGAMP (cyclic GMP-AMP), 3′,3′-cGAMP, and c-di-GMP (cyclic di-GMP) were from Invivogen.

ISD and cGAMP Transfections—ISD was transfected into THP-1 cells (typically 400,000 cells per ml in 2 ml of culture medium in a 3.5-cm plate) or HaCaT (90% confluent) using a 1:1 ratio of DNA (typically 5 μg) to Lipofectamine 2000 (5 μl) as recommended by Invitrogen. Where indicated, cells were irradiated with UV radiation 20–30 min before transfection with ISD. Transfection with 2′,3′-cGAMP, 3′,3′-cGAMP, and c-di-GMP was performed in a similar manner using Lipofectamine 2000. Unless otherwise indicated, cells were harvested 3.5–4 h after transfection, pelleted by centrifugation (1,600 × *g*, 4 min), washed with PBS, and then lysed for 10 min on ice in 50 mM Tris-HCl, pH 7.4, 150 mM NaCl, 0.5% Nonidet P-40 containing 0.1 mM PMSF, 1 mM DTT, 10 mM NaF, 1 mM Na_2VO_3, and 10 mM glycerophosphate. Soluble lysates were prepared by centrifugation at 14,000 × *g* for 10 min at 4 °C, separated by SDS-PAGE, and transferred to nitrocellulose membranes for immunoblotting. Dimerization of IRF3 was performed using native PAGE as previously described (34).

Immunoblotting—Antibodies used for immunoblotting included anti-phospho-RPA2 (Ser-33) (catalogue no. A300-246A) from Bethyl Laboratories, anti-XPB (catalogue no. sc-293), anti-Chk1 (sc-8408), anti-IRF3 (sc-9082), and anti-HA (sc-805) from Santa Cruz Biotechnology, and anti-phospho-IRF3 (Ser-396; #4947), anti-phospho-TBK1 (Ser-172; #5483), anti-TBK1 (#3504), anti-STING (#13647), anti-phospho-ULK1 (Ser-555; #5869), anti-ULK1 (#8054), anti-phospho-AMPKα (Thr-172; #2535), anti-AMPKα (#5832), anti-phospho-LKB1 (Ser-428; #3482), anti-AMBRA1 (#12250), anti-PARP (#9542), anti-phospho-Chk1 (Ser-345; #2348), anti-cleaved caspase-3 (#9661), anti-phospho-Chk2 (T68; #2661), anti-phospho-Chk1 (Ser-296; #2349), anti-phospho-p44/p42 MAPK (ERK1/2) (Thr-202/Tyr-204; #4370), anti-phospho-MAPKAPK-2 (Thr-334; #3041), anti-phospho-c-Jun (Ser-63; #9261), and anti-phospho-DNA-PK (Ser-2056; #4215) from Cell Signaling Technology. Secondary antibodies included horseradish peroxidase-linked anti-mouse and anti-rabbit IgG (catalogue no. NA931V and NA934V) from GE Healthcare. Chemiluminescence was visualized with Clarity Western ECL substrate (Bio-Rad) or Amersham Biosciences ECL Advance Substrate (GE Healthcare) using a Molecular Imager Chemi-Doc XRS+ system (Bio-Rad). Chemiluminescent signals were quantified using ImageQuant software (GE Healthcare). For each treatment condition the phospho-IRF3 (IRF3-P) signals were normalized to total IRF3 levels and then normalized to the highest IRF3-P/IRF3 signal ratio for each blot (which was set to an arbitrary value of 100). All experiments were repeated at least twice, and the average and S.E. calculated for each treatment.

RNA Interference—Lentiviral DNA particles were generated in HEK293T cells by co-transfection of the appropriate pLKO.1 vector with the packaging plasmid psPAX2 and the envelope plasmid pMD2.G with Lipofectamine 2000. Empty and XPA shRNA-containing pLKO.1 plasmids were from the Open Biosystems TRC1 shRNA library (35). THP-1 cells were infected with lentivirus in the presence of 8 μg/ml Polybrene, incubated for 24 h, and then selected with puromycin. siGENOME Non-targeting siRNA Pool #1 and ON-TARGETplus Human ULK1 siRNA SMART-pool (Dharmacon) were transfected into THP-1 cells using Lipofectamine RNAiMax (Invitrogen). Cells were transfected twice with siRNAs (40 nM) over a period of 48 h. Cells were pelleted and resuspended at 400,000 cells per ml in fresh medium before transfection with ISD.

Measurement of Excision Repair—UV-irradiated cells were lysed using a modified method of Hirt (33, 36–38). Briefly, after centrifugation and washing of UV-irradiated cells with cold PBS, the cell pellets were resuspended in 10 mM Tris-HCl, pH 8, 10 mM EDTA, and 1% SDS. NaCl was added to a final concentration of 1 M, and cells were incubated on ice for 1 h. Hirt lysates were then prepared by centrifugation (14,000 × *g*, 30

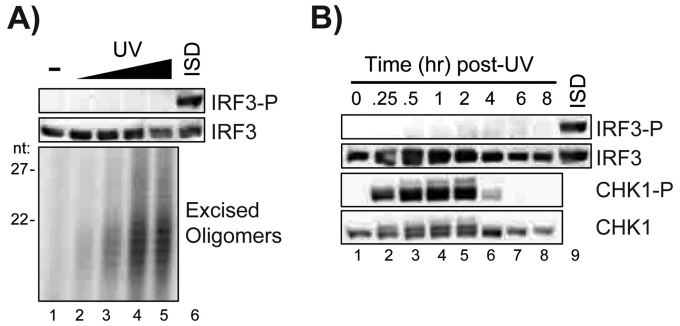

FIGURE 1. **UV radiation does not directly activate IRF3.** *A*, THP-1 monocytes were irradiated with increasing fluences of UV radiation (0, 10, 30, 100, and 300 J/m^2) or were transfected with ISD (2.5 μg/ml). Cells were harvested after 3.5 h and processed for detection of the excised oligonucleotide products of nucleotide (*nt*) excision repair and the phosphorylation of IRF3 on Ser-396. *B*, THP-1 monocytes were exposed to 100 J/m^2 of UV radiation and then harvested after the indicated periods of time. Cell lysates were prepared and analyzed with the indicated antibodies. Phospho-Chk1 (Ser-345) antibody was used as a positive control to show a cellular response to UV radiation. As an additional control, cells were transfected with ISD as described in *A*.

min, 4 °C) and digested with proteinase K for 30 min at 60 °C. After phenol-chloroform extraction and ethanol precipitation, the samples were resuspended in 10 μl of 10 mM Tris-HCl, pH 8.5. Half of the resuspended DNA was 3′-end labeled in a 10-μl reaction containing 6 units of terminal deoxynucleotidyltransferase (TdT; New England Biolabs), 0.25 mM $CoCl_2$, and 3′-[α-^{32}P]ATP (cordycepin 5′-triphosphate; PerkinElmer Life Sciences) in 1× TdT buffer (New England Biolabs) for 1 h at 37 °C. After phenol-chloroform extraction and ethanol precipitation, the radiolabeled excised oligonucleotides were separated on urea-containing polyacrylamide gels and then detected with phosphorimaging. Radiolabeled oligonucleotides of known length were resolved on all gels as size markers. Excision repair activity was quantified using ImageQuant 5.2 software (GE Healthcare) as previously described (33).

RESULTS

UV Radiation Does Not Directly Activate IRF3—Although exposure to UV wavelengths of sunlight is known to exacerbate the symptoms of the autoimmune disorder SLE (1–3), the molecular mechanisms that are responsible for this effect and the relative roles of the innate and adaptive immune systems are not clear. Because the protein STING has emerged as a critical regulator of innate immunity (6–8), we therefore considered the possibility that UV light may specifically modulate STING-dependent innate immune signaling.

To test this hypothesis, THP-1 monocytes were exposed to increasing amounts of UV radiation and then harvested to examine STING activation. In response to specific immune stimuli such as cytosolic DNA, activated STING functions as a scaffold or adaptor protein to facilitate the phosphorylation of IRF3 on Ser-396 by the upstream kinase TBK1 (22). As a positive control for activation of the STING-IRF3 pathway in these experiments, we transfected cells with a 45-bp-long dsDNA termed interferon-stimulatory DNA (ISD) for its ability to induce interferon expression in responsive cells (23). As shown in Fig. 1*A*, although ISD induced a robust response (*lane 6*), IRF3 phosphorylation was not observed in the UV-irradiated cells even at high doses of UV that saturate the ability of the nucleotide excision repair system to remove UV photoproducts from genomic DNA (Fig. 1*A*, *bottom panel*).

We next performed time course experiments to monitor the kinetics of IRF3 phosphorylation after UV irradiation. Although UV induced rapid phosphorylation of the DNA damage checkpoint kinase Chk1, there was no evidence of IRF3 phosphorylation at any time point after irradiation (Fig. 1*B*). Similarly, when we treated THP-1 cells with the UV-mimetic AAF, we did not observe detectable levels of IRF3 phosphorylation (data not shown).

These results indicate that the exposure of cultured human cells to UV alone is not sufficient to activate IRF3. Because IRF3 phosphorylation is essential for downstream innate immune signaling responses to cytosolic DNA (23), we conclude that UV does not directly induce a STING/IRF3-mediated innate immune response.

UV Stimulates TBK1-IRF3 Signaling in Response to Cytosolic DNA—In addition to sunlight exposure, viral and microbial infections are additional risk factors for SLE (39, 40) and may result in the release of pathogen-derived DNA into the cytosol of infected cells. Whether exposures to UV wavelengths of sunlight may work in concert with microbial infections to impact the symptoms of autoimmune disorders is not known.

We, therefore, sought to mimic such a scenario by introducing DNA into the cytosol of UV-irradiated cells. THP-1 cells were irradiated with UV and then transfected with increasing amounts of ISD. As shown in Fig. 2*A*, under conditions where limiting amounts of ISD were introduced into cells, UV exposure enhanced IRF3 phosphorylation and, to a lesser extent, the phosphorylation of the upstream IRF3 kinase TBK1, which can undergo STING-dependent autophosphorylation (22). Furthermore, the level of IRF3 phosphorylation potentiated by UV in ISD-transfected cells was dependent on UV dose and became saturated at ~100 J/m^2 (Fig. 2*B*), which is a dose that saturates nucleotide excision repair capacity in THP-1 cells (Fig. 1*A*). Moreover, time course experiments showed that UV affected the amplitude of IRF3 phosphorylation but not the general kinetics of the response following ISD administration (Fig. 2*C*).

Additional experiments aimed at determining how the timing of UV exposure relative to the exposure of the cytosol to DNA affected this response showed that UV exposures up to 1 h before or after transfection with ISD led to maximal stimulation of IRF3 phosphorylation but that prolonged incubation times of >1–2 h after irradiation and before ISD transfection instead inhibited TBK1-IRF3 signaling in response to ISD (data not shown). These results indicate that an optimal window of exposure exists under which UV can enhance TBK1-IRF3 signaling in response to cytosolic DNA.

A quantitative analysis of the response of THP-1 monocytes to UV under optimized conditions of ISD concentration, UV dose, and treatment time is presented in Fig. 2*D*. These data show that the phosphorylation of IRF3 was completely ISD-dependent and was stimulated 3–5-fold by UV exposure. To confirm these observations in another cell line of physiological relevance to sunlight UV exposure, we irradiated HaCaT keratinocytes with UV and then transfected the cells with ISD. As shown in Fig. 2*E*, IRF3 phosphorylation was enhanced 4–5-

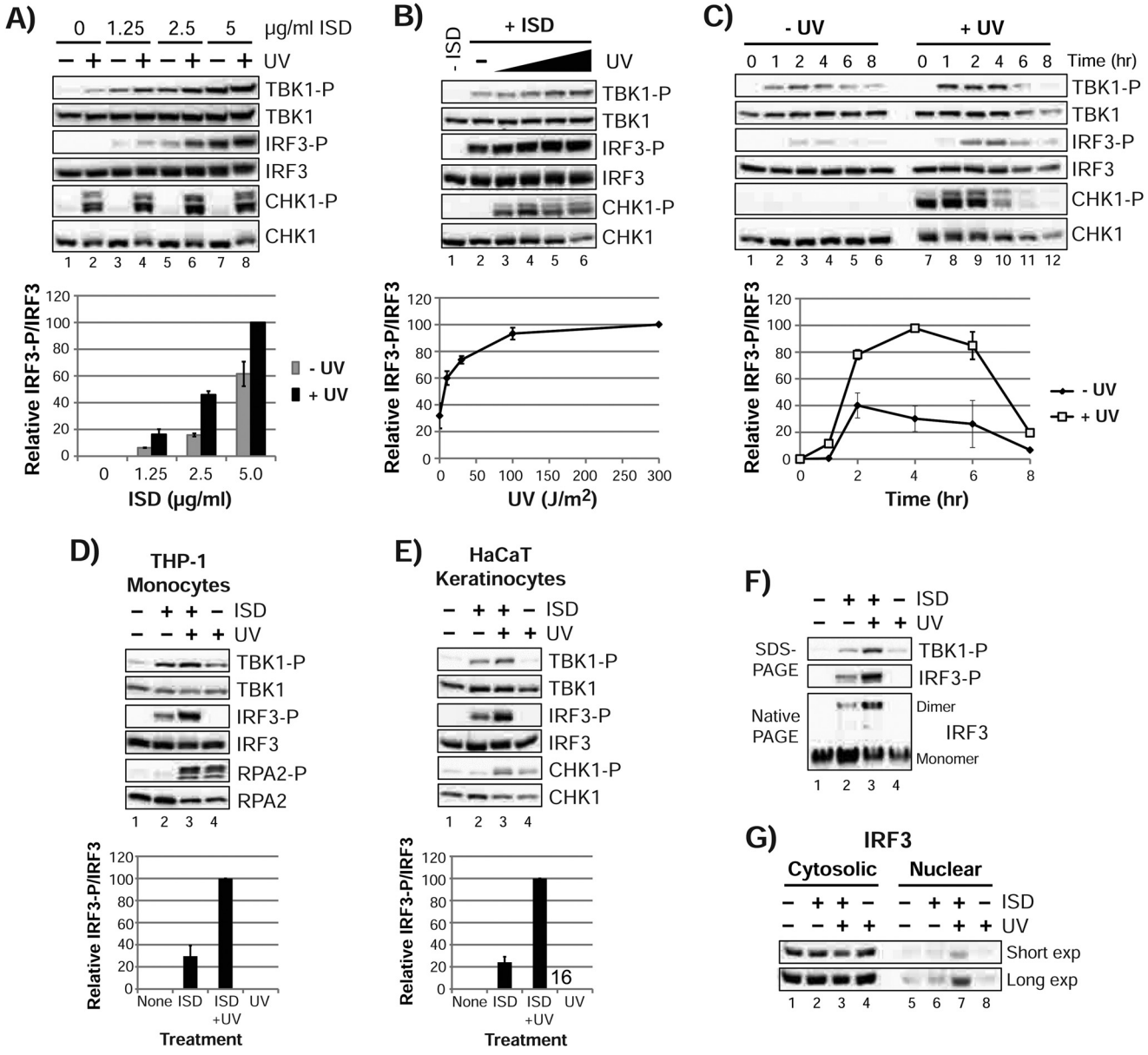

FIGURE 2. **UV stimulates cytosolic DNA-dependent TBK1-IRF3 signaling.** *A*, THP-1 monocytes were irradiated with 50 J/m^2 of UV and then transfected with the indicated amounts of ISD. Cell lysates were prepared 3.5 h after transfection and analyzed by immunoblotting. The IRF3-P and IRF3 signals were quantified by densitometry. The IRF3-P/IRF3 ratio was determined for each condition and then normalized to the highest value for each blot, which was set to an arbitrary value of 100. The graphs represent the average and S.E. from two independent experiments. *B*, THP-1 cells were exposed to increasing fluences of UV (0, 10, 30, 100, and 300 J/m^2), transfected with 2.5 μg/ml ISD and then harvested 3 h later for immunoblot analysis. IRF3-P/IRF3 signals were quantified as described in *A*. *C*, THP-1 cells were irradiated with 100 J/m^2 of UV and then transfected with 2.5 μg/ml ISD 20 min later. Cells were harvested at the indicated time points and analyzed by immunoblotting. IRF3-P/IRF3 signals were quantified as described in *A*. *D*, THP-1 monocytes were irradiated with UV (100 J/m^2) and/or transfected with ISD (2.5 μg/ml) as indicated. Cells were harvested after 3.5–4 h and analyzed by immunoblotting. Quantified data show the average and S.E. from nine independent experiments. *E*, HaCaT cells were treated as in *D*. The graph shows the average and S.E. from three independent experiments. *F*, THP-1 cells were treated as in *D* except that cell lysates were analyzed by SDS-PAGE and native-PAGE before immunoblot analysis. *G*, THP-1 cells treated as in *D* were fractionated to separate the cytosolic and nuclear material before SDS-PAGE and immunoblot analysis.

fold by UV in ISD-transfected keratinocytes but was not impacted by UV in the absence of ISD.

Phosphorylation of IRF3 is associated with protein dimerization and entry into the nucleus, where it acts as a transcription factor for genes involved in immunity, inflammation, and apoptosis (23–26, 34). We, therefore, used native-PAGE to monitor the dimerization of IRF3 and observed that IRF3 dimerization was ISD-dependent and further stimulated by UV (Fig. 2*F*). Similarly, the amount of IRF3 found in the nuclear fraction of cells was increased in ISD-transfected cells exposed to UV (Fig. 2*G*). Thus, using several different biochemical readouts for IRF3 activation, we conclude that UV stimulates IRF3 activation in a manner that is dependent upon the introduction of cytosolic DNA into cells.

UV-mimetics Stimulate Cytosolic DNA-dependent TBK1-IRF3 Signaling—UV radiation results in the formation of photoproducts in genomic DNA that interfere with gene transcription and other aspects of DNA metabolism. However, UV also causes damage to other cellular biomolecules that may modulate the cellular response to cytosolic DNA. Thus, to determine

whether damage to cellular DNA is responsible for potentiating TBK1-IRF3 signaling in response to transfected DNA, we treated cells with the UV-mimetic chemical carcinogens BPDE and AAF. As shown in Fig. 3*A*, BPDE and AAF stimulated ISD-dependent IRF3 phosphorylation to a similar extent as UV. Moreover, the effects of AAF and BPDE were found to be dose-dependent (Fig. 3, *B* and *C*).

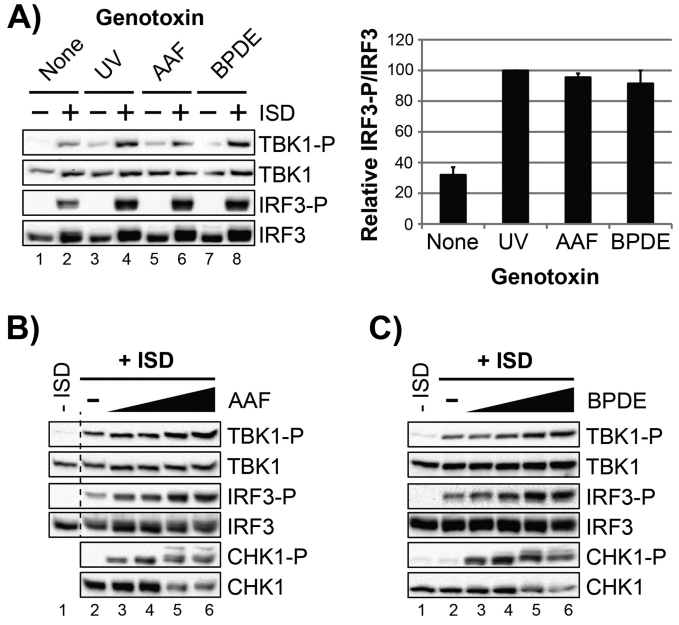

FIGURE 3. **The UV-mimetic chemical carcinogens BPDE and AAF potentiate cytosolic DNA-dependent TBK1-IRF3 signaling.** *A*, THP-1 monocytes were exposed to the indicated genotoxin (100 J/m^2 UV, 10 μM AAF, or 10 μM BPDE) 20 min before transfection with ISD. Cells were harvested 3.5 h later and processed for immunoblot analysis. The graph shows the average (+S.E.) IRF3-P/IRF3 signal in ISD-transfected cells exposed to the indicated genotoxins from two independent experiments. *B*, THP-1 cells were exposed to increasing concentrations of AAF (0, 0.3, 1, 3, and 10 μM), transfected with ISD for 3.5 h, and then analyzed by immunoblotting. *C*, THP-1 cells were exposed to increasing concentrations of BPDE (0, 0.3, 1, 3, and 10 μM) and are described in *B*.

UV, AAF, and BPDE all induce formation of "bulky adducts" in DNA that are removed from the genome by the nucleotide excision repair system (41–43), which indicated that a cellular response to these types of lesions is responsible for the effect of UV and UV-mimetic agents on the stimulation of cytosolic DNA-dependent TBK1-IRF3 signaling. To examine whether the repair of these forms of DNA damage is required to potentiate the cellular response to cytosolic DNA, we generated THP-1 cell lines that stably expressed shRNAs against the essential nucleotide excision repair factor XPA. Although XPA protein expression was reduced by >95% in two independent cell lines (Fig. 4*A*), which reduced the rate of nucleotide excision repair by 4–5-fold (Fig. 4*B*), XPA knockdown did not affect the stimulation of ISD-dependent IRF3 activation by UV (Fig. 4, *C* and *D*). We conclude that an intact nucleotide excision repair system is not required for UV and UV-mimetics to potentiate TBK1-IRF3 signaling in response to cytosolic DNA.

These lesions also activate a number of cell signaling pathways that govern various cellular responses to DNA damage and associated genomic stress (44, 45). However, the use of chemical inhibitors of several DNA damage response kinases and mitogen-activated protein (MAP) kinases that are known to be activated after UV irradiation showed that the kinase activities of ATR, Chk1, ATM, DNA-PK, p38, JNK, and MEK1/2 were not responsible for the effect of UV on STING-dependent IRF3 activation by cytosolic DNA (data not shown).

Furthermore, additional experiments demonstrated that UV potentiated the cytosolic DNA response in nocodazole-arrested mitotic THP-1 cells and in serum-starved quiescent HaCaT cells (data not shown), which indicates that the effect of UV on IRF3 activation is independent of the cell cycle phase.

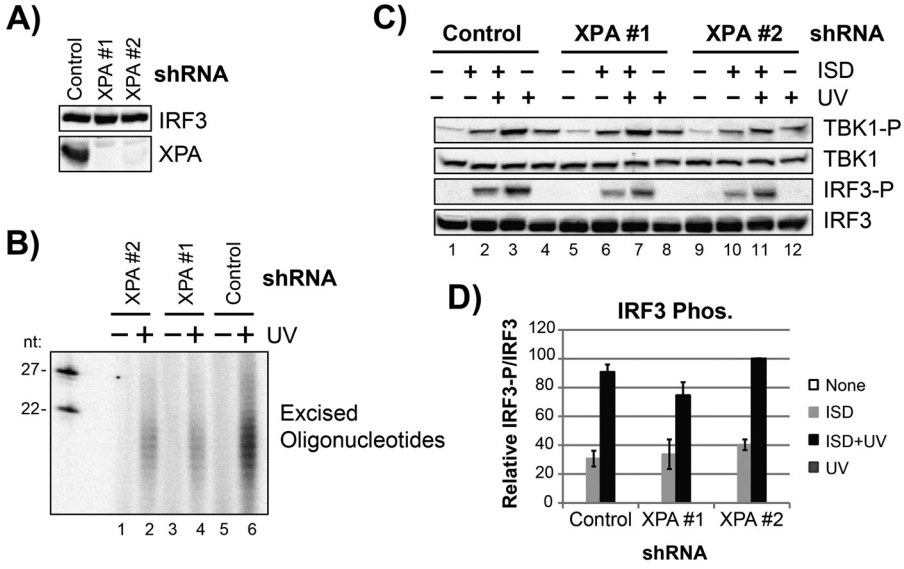

FIGURE 4. **UV stimulation of cytosolic DNA-dependent TBK1-IRF3 signaling is independent of nucleotide excision repair.** *A*, lysates from THP-1 monocytes stably expressing XPA shRNA-expressing vectors or an empty vector (control) were analyzed by immunoblotting. *B*, the indicated THP-1 cell lines were exposed to UV (100 J/m^2) and harvested 3.5 h later for analysis of nucleotide excision repair. Excised oligomers were radiolabeled, electrophoresed on a denaturing gel, and visualized with by phosphorimaging. *C*, the indicated cells lines were exposed to UV radiation and/or transfected with ISD as indicated. Lysates were analyzed by immunoblotting. *D*, quantitative analysis of experiments performed as in *C*. The *graph* shows the average and S.E. from three independent experiments.

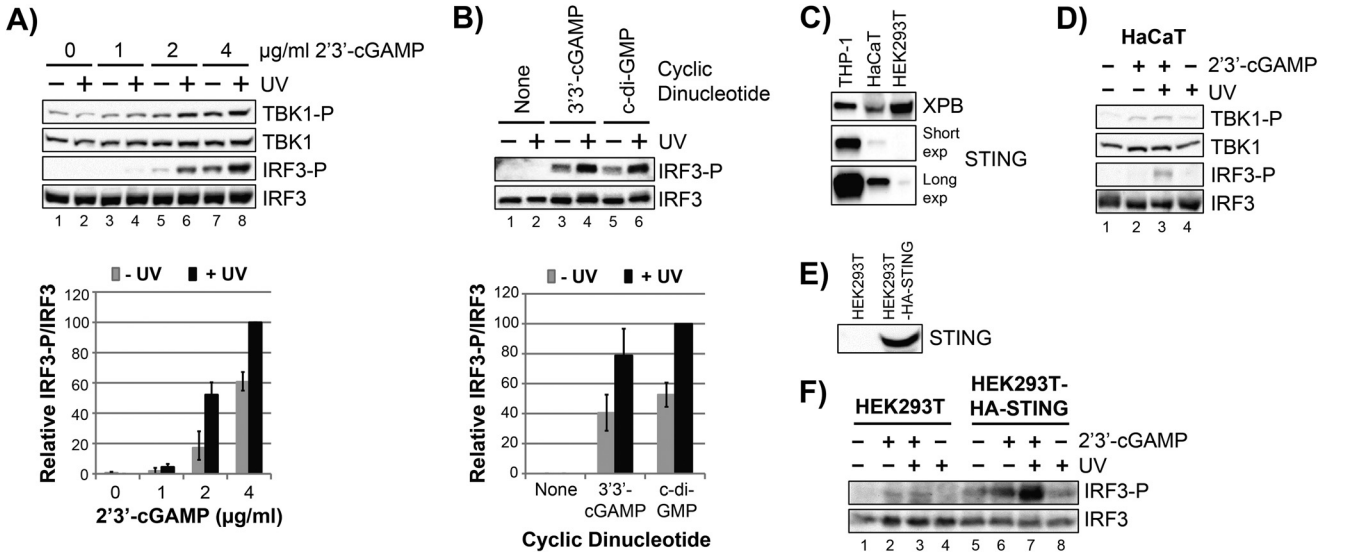

FIGURE 5. **Stimulation of TBK1-IRF3 signaling by cyclic dinucleotides is STING-dependent.** *A*, THP-1 monocytes were irradiated or not with UV (100 J/m^2) and then transfected with the indicated concentration of 2′,3′-cGAMP. Cell lysates were prepared 3 h later and analyzed by immunoblotting. The graph shows the average IRF3-P/IRF3 signal (with S.E.) from three independent experiments. *B*, THP-1 cells were treated as in *A* except that 3′,3′-cGAMP or c-di-GMP were transfected into the cells. The *graph* shows the average and S.E. from three to four independent experiments. *C*, cell lysates from the indicated cell lines was analyzed by immunoblotting with the indicated antibodies. *D*, HaCaT cells were treated as shown, and cell lysates were examined by immunoblotting. *E*, lysates from HEK293T or HEK293T cells stably expressing an HA epitope-tagged STING construct were analyzed by immunoblotting with an anti-STING antibody. *F*, the indicated cells were irradiated with UV (100 J/m^2) and/or transfected with 2′,3′-cGAMP (12 μg/ml) as indicated. Cell lysates were prepared 3.5 h later and analyzed by immunoblotting.

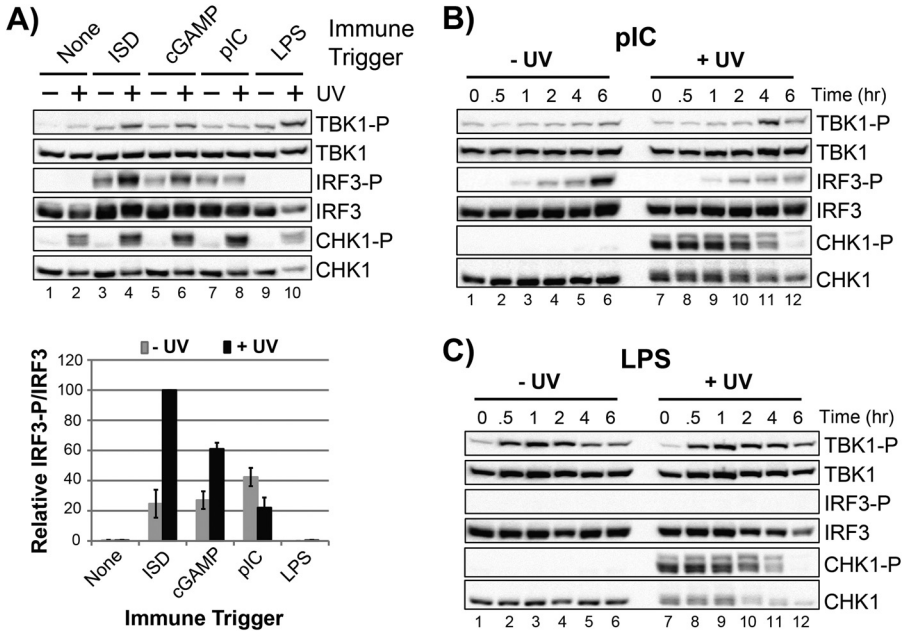

FIGURE 6. **UV does not stimulate TBK1-IRF3 signaling in response to RNA or LPS.** *A*, THP-1 cells were irradiated with UV and treated with the indicated trigger of immune signaling. Cell lysates were prepared and analyzed by immunoblotting. The graph shows the average (with S.E.) IRF3-P/IRF3 signal for each condition. *B*, THP-1 cells were exposed or not to UV and then transfected with pIC. Cells were harvested at the indicated time points and analyzed by immunoblotting. *C*, cells were processed as described in *B* except that LPS was added to the culture medium.

UV Stimulates TBK1-IRF3 Signaling in Response to Cyclic Dinucleotides—To better understand the mechanism by which UV and UV-mimetic chemical carcinogens impact IRF3 activation, we next determined whether UV affected the cellular response to other activators of innate immune signaling. We first investigated the cyclic dinucleotide 2′,3′-cGAMP, which is produced by the enzyme cGAS upon binding to cytosolic DNA (10, 11, 13, 14). Although STING has a low affinity for DNA, its activation in response to cytosolic DNA is thought to occur instead through binding to the intermediate signaling molecule 2′,3′-cGAMP (17), which alters the conformation of STING and allows it to mediate phosphorylation of IRF3 by TBK1 (5, 20, 21). Exogenous 2′,3′-cGAMP can, therefore, be introduced into cells to directly activate the STING-TBK1/IRF3 pathway and bypass the need for cGAS or cytosolic DNA (9). Thus, we next asked whether UV affects the innate immune response to 2′,3′-cGAMP in a similar manner as for cytosolic DNA.

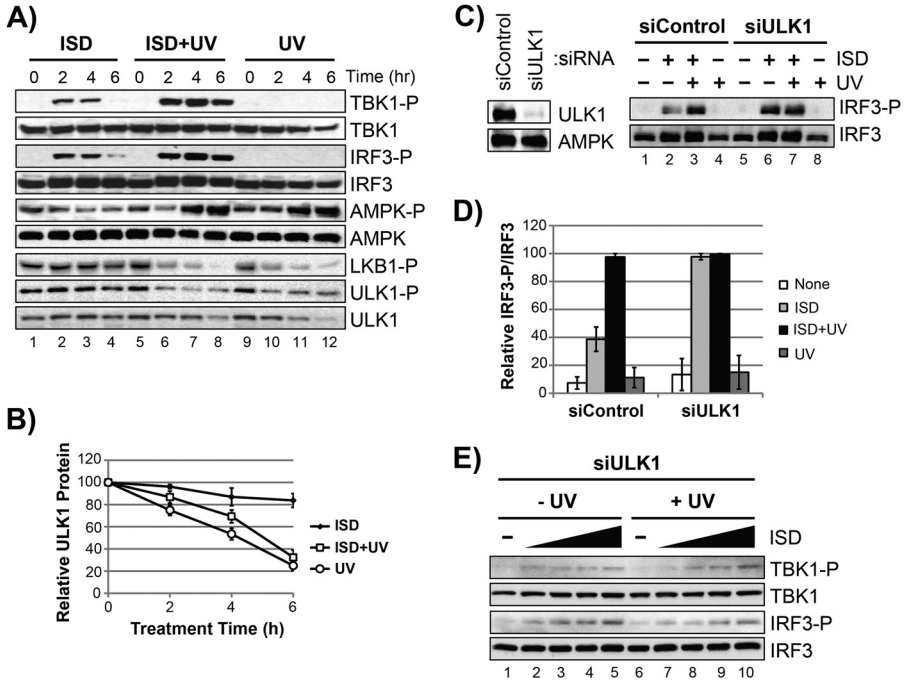

FIGURE 7. **UV modulates LKB1-AMPKα-ULK1 signaling and impacts ULK1 protein levels.** *A*, THP-1 cells were treated as shown and then harvested at the indicated time points for immunoblot analysis. *B*, ULK1 protein level at each time point was quantified from at least three experiments described in *A*. Signals were normalized to the ULK1 signal at time 0. *Error bars* represent S.E. *C*, THP-1 monocytes were transfected with the indicated siRNAs as described under in "Experimental Procedures" and then treated with UV and or ISD. *D*, the average IRF3-P/IRF3 signals (with S.E.) from two independent experiments is presented in the graph. *E*, THP-1 monocytes transfected with ULK1 siRNA were exposed or not to UV radiation and then transfected with increasing concentrations of ISD (0, 0.625, 1.25, 2.5, or 5 μg/ml). Cells were harvested after 3.5 h and analyzed by immunoblotting.

Non-irradiated and UV-irradiated THP-1 cells were, therefore, transfected with increasing amounts of cGAMP and then analyzed for stimulation of TBK1-IRF3 signaling. As shown in Fig. 5*A*, the level of IRF3 phosphorylation was stimulated by UV at each concentration of 2′,3′-cGAMP. Thus, UV stimulates IRF3 activation after the administration of both cytosolic DNA (ISD) and 2′,3′-cGAMP.

Other pathogen-derived cyclic dinucleotides, including 3′,3′-cGAMP and c-di-GMP, are released into the cytosol of mammalian cells upon infection with specific microbes and have been shown to bind and stimulate STING (16, 18, 19, 46). As shown in Fig. 5*B*, we found that UV stimulated the level of IRF3 phosphorylation ~2–2.5-fold in response to both of these cyclic dinucleotides.

Because IRF3 activation by cytosolic DNA and cyclic dinucleotides is dependent upon the expression of STING, we next examined the protein levels of STING in different human cell lines. Consistent with previous reports (10), STING protein expression was readily detectable in THP-1 monocytes but was nearly absent in HEK293T cells (Fig. 5*C*). Although less abundant than in THP-1 cells, STING protein was clearly evident in HaCaT keratinocytes, which is supported functionally by the ability of HaCaT cells to respond to cytosolic DNA (Fig. 2*E*). Furthermore, when we transfected UV-irradiated HaCaT keratinocytes with low amounts of 2′,3′-cGAMP, we observed that UV exposure promoted cGAMP-dependent IRF3 phosphorylation (Fig. 5*D*). We conclude that UV stimulates IRF3 phosphorylation in response to both cytosolic DNA and cyclic dinucleotides in keratinocytes and other human cells.

Transfection of HEK293T cells (which express very low levels of STING) with 2′,3′-cGAMP led to only a small induction of IRF3 phosphorylation. However, when we stably expressed an HA-tagged STING construct in HEK293T cells (Fig. 5*E*), we observed a much more robust response to 2′,3′-cGAMP that was further enhanced by exposure of the cells to UV. We conclude that UV enhances IRF3 activation in response to both cytosolic DNA and cyclic dinucleotides and that this response is dependent on the expression of STING.

UV Does Not Stimulate TBK1-IRF3 Signaling in Response to RNA or LPS—TBK1 and IRF3 are also utilized in a STING-independent but MAVS-dependent signaling pathway that responds to viral RNA and that similarly results in IRF3 phosphorylation and activation (47). Thus, to determine whether the effect of UV on TBK1-IRF3 signaling is specific for the cytosolic DNA/cyclic dinucleotide-STING-dependent pathway, we transfected non-irradiated and UV-irradiated cells with ISD, 2′,3′-cGAMP, or the viral RNA mimic pIC and then monitored the phosphorylation status of TBK1 and IRF3. As an additional control, we also added the immune trigger and bacterial wall component lipopolysaccharide (LPS) to the culture medium of non-irradiated and UV-irradiated cells. As shown in Fig. 6*A*, IRF3 phosphorylation was enhanced by UV in cells that were transfected with ISD or cGAMP but not in cells that were stimulated with pIC or LPS.

Because the kinetics of innate immune signaling may be different with pIC and LPS than with DNA and cGAMP, we also performed time course experiments after stimulation with pIC and LPS. Although pIC induced a time-dependent increase in IRF3 phosphorylation in non-irradiated cells, the response was partially abrogated in UV-irradiated cells (Fig. 6*B*). IRF3 phosphorylation was not observed at any time point after LPS administration either in the absence or presence of UV (Fig.

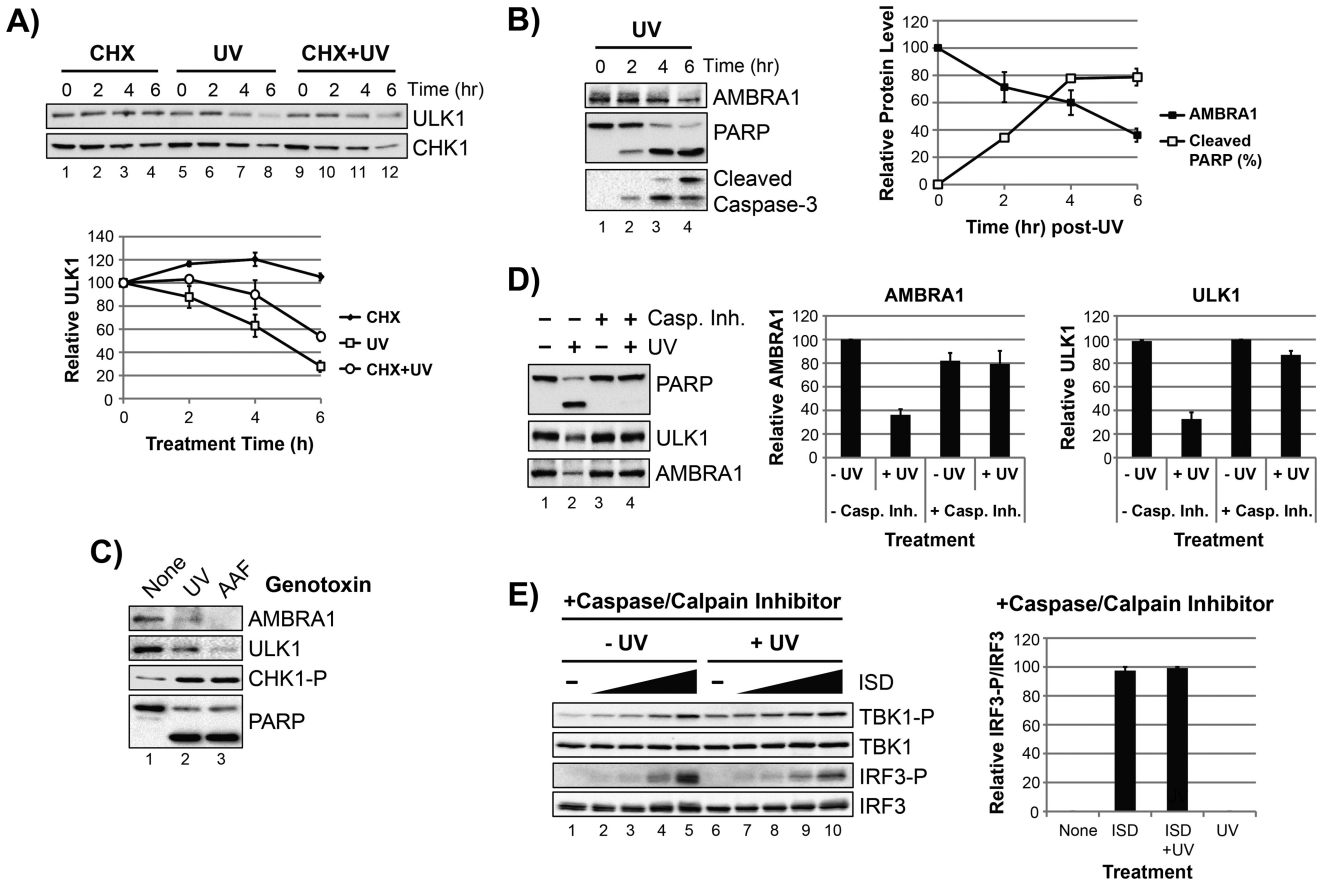

FIGURE 8. **UV-induced apoptotic signaling destabilizes ULK1 and AMBRA1 and is required for UV to potentiate STING-dependent IRF3 activation.** *A*, THP-1 cells were preincubated or not for 15 min with cycloheximide (*CHX*) before UV irradiation. Cells were harvested at the indicated time points. Cell lysates were prepared and then analyzed by immunoblotting with anti-ULK1 or anti-Chk1 antibodies. *B*, THP-1 monocytes were exposed to UV (100 J/m^2) and then harvested at the indicated time points. Cell lysates were prepared and examined by immunoblotting. The *graph* shows the average level of AMBRA1 protein and the percentage of cleaved poly(ADP-ribose) polymerase (*PARP*; relative to full-length plus cleaved) at each time point relative to the 0-h time point. *Error bars* represent the S.E. from two to five independent experiments. *C*, THP-1 monocytes were exposed to UV (100 J/m^2) or AAF (20 μM) and then incubated for 6 h. Cell lysates were analyzed by immunoblotting. *D*, THP-1 monocytes were preincubated for 15 min with caspase and calpain inhibitors (abbreviated *Casp. Inh.*) before UV irradiation. Cells were harvested 6 h later, and cell lysates were analyzed by immunoblotting. The *graphs* show the relative levels of AMBRA1 and ULK1 protein under each condition, with the signals normalized to the highest value for each blot (average and S.E. from two to six independent experiments). *E*, THP-1 monocytes treated with caspase and calpain inhibitors were irradiated or not with UV and then transfected with increasing amounts of ISD (0, 0.38, 0.63, 1.25, 2.5 μg/ml). Cells were harvested after 3.5 h and analyzed by immunoblotting. The *graph* shows the average relative IRF3-P/IRF3 signal (using 2.5 μg/ml ISD) from two independent experiments. *Error bars* show the S.E.

6*C*). These results lead us to conclude that the effect of UV on TBK1-IRF3 signaling is specific to the STING-dependent pathway that responds to cytosolic DNA and cyclic dinucleotides.

UV Modulates LKB1-AMPKα-ULK1 Signaling and Impacts ULK1 Protein Levels—We next considered that UV may affect a pathway that directly controls STING activity. Interestingly, STING was recently shown to be negatively regulated by a signaling cascade comprising the kinases LKB1-AMPKα-ULK1 (liver kinase B1, AMP-activated protein kinase, and Unc51-like kinase 1, respectively), which ultimately results in the phosphorylation of STING by ULK1 (32) and which interferes with the activation of IRF3. Thus, the activation of ULK1 through LKB1 and AMPK is thought to dampen or turn off TBK1-IRF3 signaling in response to cytosolic DNA and cyclic dinucleotides (32).

We, therefore, next examined the status of the LKB1-AMPKα-ULK1 signaling cascade after ISD transfection in the absence and presence of UV irradiation by monitoring the phosphorylation status of the pathway kinases. Consistent with a previous report (32), we observed that ISD induced a modest reduction in AMPKα phosphorylation under our conditions (Fig. 7*A*, *lanes 1–4*). In contrast, the phosphorylation status of AMPKα increased in UV-irradiated cells regardless of ISD transfection (Fig. 7*A*, *lanes 5–12*). Moreover, UV also induced a dramatic reduction in the phosphorylation status of LKB1. These results indicate that UV alters LKB1-AMPKα-ULK1 signaling and may prevent it from responding normally to ISD (Fig. 7*A*, *lanes 5–12*). However, we also noted a dramatic loss in total ULK1 protein levels in UV-irradiated cells (Fig. 7*A*), such that ULK1 protein levels decreased by nearly 80% within 6 h after UV irradiation (Fig. 7*B*).

The loss of ULK1 after UV would be expected to prevent ULK1 from phosphorylating and negatively regulating STING. Thus, loss of this negative regulator should result in increased phosphorylation of IRF3 by TBK1. To determine whether UV potentiation of IRF3 activation in response to cytosolic DNA is dependent on ULK1, we next used RNA interference to reduce ULK1 expression in THP-1 cells. Consistent with a recent report (32), knockdown of ULK1 led to elevated IRF3 phosphorylation after ISD transfection (Fig. 7*C*, compare *lanes 2* and *6*). Furthermore, although UV stimulated the effect of cytosolic

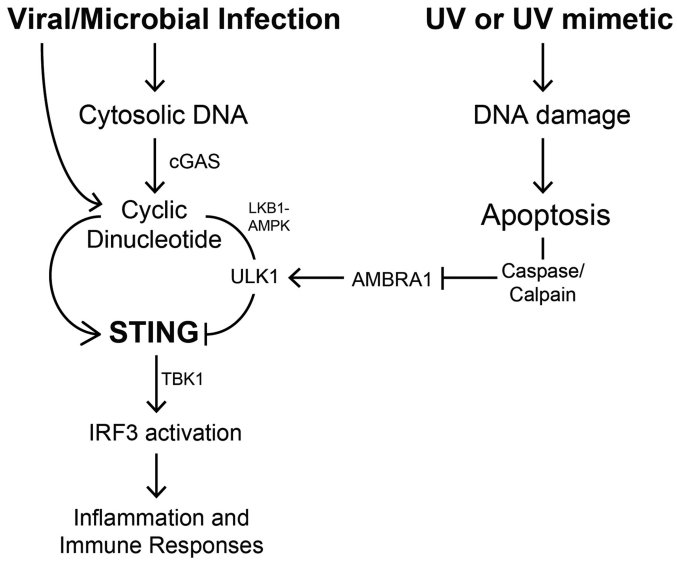

FIGURE 9. **Model for the role of UV radiation in the modulation of STING-dependent IRF3 activation.** Cyclic dinucleotides (3′,3′-cGAMP and c-di-GMP) released during microbial infection or 2′,3′-cGAMP produced by cGAS upon binding to cytosolic DNA following viral or microbial infection stimulate STING to mediate phosphorylation and activation of IRF3 by TBK1, which results in inflammatory and immune responses. These cyclic dinucleotides also stimulate an LKB1-AMPKα-ULK1 signaling pathway that inhibits the STING pathway. In cells exposed to UV or a UV-mimetic, high levels of DNA damage induce apoptotic signaling (mediated by caspases and calpains) that destabilize AMBRA1 and ULK1. This loss of the STING negative regulator ULK1 results in an amplified response to cytosolic DNA and cyclic dinucleotides.

DNA on IRF3 phosphorylation in cells transfected with a control siRNA (Fig. 7*C*, *lanes 2* and *3*), UV did not affect the response in cells depleted of ULK1 (Fig. 7*C*, *lanes 6* and *7*). Quantitation of this experimental approach is provided in Fig. 7*D* and shows that ISD-induced IRF3 phosphorylation administration is elevated in both the absence and presence of UV when ULK1 is depleted from the cells.

To ensure that the signaling pathway leading to ISD-induced IRF3 activation is not simply saturated under our experimental conditions in ULK1-depleted cells, we transfected varying amounts of ISD into cells depleted of ULK1 via RNA interference and then monitored TBK1 and IRF3 phosphorylation. As shown in Fig. 7*E*, UV failed to enhance the effect of ISD on IRF3 activation at each concentration of ISD in cells transfected with ULK1 siRNAs. These results demonstrate that UV potentiation of IRF3 activation by cytosolic DNA only takes place when ULK1 is present in cells.

UV-induced Apoptotic Signaling Destabilizes ULK1 and AMBRA1—We next sought to determine the mechanism by which ULK1 protein levels decrease upon UV exposure. Treatment with cycloheximide to block new protein synthesis showed that ULK1 protein has a relatively long half-life in THP-1 cells (Fig. 8*A*), which indicates that the loss of ULK1 protein upon UV irradiation may be through an active post-translational or proteolytic process and not likely not due to simple inhibition of ULK1 transcription or translation.

ULK1 protein stability and kinase activity have been shown to be influenced by the autophagy regulatory protein AMBRA1 (autophagy/beclin-1 regulator 1) (48). Interestingly, we observed that AMBRA1 protein levels decreased after UV irradiation (Fig. 8*B*). Thus, the decrease in ULK1 protein levels and increase in STING activity may be associated with the UV-mediated loss of AMBRA1.

AMBRA1 has been reported to be degraded by a caspase- and calpain-mediated pathway in response to apoptotic stimuli (49–51), and we observed that the loss of ULK1 and AMBRA1 after UV irradiation coincided with the activation of apoptotic signaling, as measured by cleavage of poly(ADP-ribose) polymerase (*PARP*) and caspase 3 (Fig. 8*B*). This correlation between activation of apoptotic signaling and loss of ULK1 and AMBRA1 was similarly observed upon treatment of THP-1 cells with the UV-mimetic AAF (Fig. 8*C*).

We, therefore, next examined how inhibition of apoptotic signaling affected the levels of ULK1 and AMBRA1 in UV-irradiated cells. As shown in Fig. 8*D*, inhibition of apoptotic signaling prevented the loss of ULK1 and AMBRA1 protein after UV irradiation.

To determine whether apoptotic signaling and the subsequent loss of ULK1 and the ULK1 regulator AMBRA1 were responsible for the UV-mediated enhancement of IRF3 phosphorylation after ISD transfection, we treated cells with caspase and calpain inhibitors before UV irradiation and transfection with ISD. As shown in Fig. 8*E*, UV was unable to stimulate IRF3 phosphorylation when apoptotic signaling was inhibited.

These results indicate that the activation of apoptotic signaling and the resulting loss of the negative STING regulator ULK1 are responsible for the stimulation of the cytosolic DNA response by UV radiation. The ultimate impact of this deregulation by UV is a potentiation of the STING-IRF3-dependent innate immune response to ISD and cyclic dinucleotides.

DISCUSSION

In this study we uncovered a novel mechanism by which UV radiation and related chemical carcinogens specifically enhance the STING-dependent innate immune response that activates the transcription factor IRF3 after exposure to cytosolic DNA and cyclic dinucleotides.

A schematic summarizing our findings is presented in Fig. 9. Cytosolic DNA or cyclic dinucleotides that arise in cells after viral or microbial infection stimulate STING, which allows STING to function as an adaptor for phosphorylation and activation of IRF3 by TBK1. These same stimuli also activate a negative regulatory pathway that leads ULK1 to phosphorylate and inactivate STING to dampen the immune response (32). Importantly, we discovered that high levels of UV radiation, which saturate DNA repair capacity (Fig. 1*A*), disrupt this negative regulation by promoting the destruction of ULK1 and the ULK1 regulator AMBRA1 in a caspase/calpain-dependent manner (Fig. 8). The result of this deregulation is an increase in STING-IRF3 activation after UV irradiation. Because IRF3 regulates the expression of a wide variety of genes, including those involved in immune signaling, inflammation, and apoptosis, future work will need to characterize how UV radiation modulates the transcription program that is controlled by IRF3.

Our observation that UV impacts an innate immune response in human keratinocytes has implications for understanding how sunlight UV exposures trigger or exacerbate disease symptoms in patients with SLE. This issue is particularly relevant in light of reported cases of SLE patients who have

experienced serious skin flare-ups of cutaneous lupus and even life-threatening lupus nephritis after sunburn or tanning (52, 53). Furthermore, our results show that UV exposure modulates a canonical response to pathogenic immune stimuli (cytosolic DNA and cyclic dinucleotides) but that UV alone does not apparently induce the STING-dependent innate immune pathway. Experimental models of autoimmunity should, therefore, consider the possibility that these two risk factors (infection and sun exposure) work in concert to impact the immune system.

Note Added in Proof—The data shown for phosphorylated Tank-binding kinase 1 (TBK1-P) expression in THP-1 monocytes after AAF treatment was not correct in the version of Fig. 3*B* that was published on March 19, 2015 as a Paper in Press. Specifically, the immunoblot image representing TBK-1P expression after BPDE treatment in Fig. 3*C* was mistakenly duplicated and reused in Fig. 3*B*. This error has been corrected. This correction does not change the interpretation of the results or the conclusions.

REFERENCES

1. Baer, R. L., and Harber, L. C. (1965) Photobiology of lupus erythematosus. *Arch. Dermatol.* **92,** 124–128
2. Epstein, J. H., Tuffanelli, D., and Dubois, E. L. (1965) Light sensitivity and lupus erythematosus. *Arch. Dermatol.* **91,** 483–485
3. Barbhaiya, M., and Costenbader, K. H. (2014) Ultraviolet radiation and systemic lupus erythematosus. *Lupus* **23,** 588–595
4. O'Neill, L. A. (2013) Immunology. Sensing the dark side of DNA. *Science* **339,** 763–764
5. Cai, X., Chiu, Y. H., and Chen, Z. J. (2014) The cGAS-cGAMP-STING pathway of cytosolic DNA sensing and signaling. *Mol. Cell* **54,** 289–296
6. Ishikawa, H., and Barber, G. N. (2008) STING is an endoplasmic reticulum adaptor that facilitates innate immune signalling. *Nature* **455,** 674–678
7. Ishikawa, H., Ma, Z., and Barber, G. N. (2009) STING regulates intracellular DNA-mediated, type I interferon-dependent innate immunity. *Nature* **461,** 788–792
8. Zhong, B., Yang, Y., Li, S., Wang, Y. Y., Li, Y., Diao, F., Lei, C., He, X., Zhang, L., Tien, P., and Shu, H. B. (2008) The adaptor protein MITA links virus-sensing receptors to IRF3 transcription factor activation. *Immunity* **29,** 538–550
9. Wu, J., Sun, L., Chen, X., Du, F., Shi, H., Chen, C., and Chen, Z. J. (2013) Cyclic GMP-AMP is an endogenous second messenger in innate immune signaling by cytosolic DNA. *Science* **339,** 826–830
10. Sun, L., Wu, J., Du, F., Chen, X., and Chen, Z. J. (2013) Cyclic GMP-AMP synthase is a cytosolic DNA sensor that activates the type I interferon pathway. *Science* **339,** 786–791
11. Zhang, X., Wu, J., Du, F., Xu, H., Sun, L., Chen, Z., Brautigam, C. A., Zhang, X., and Chen, Z. J. (2014) The cytosolic DNA sensor cGAS forms an oligomeric complex with DNA and undergoes switch-like conformational changes in the activation loop. *Cell Rep.* **6,** 421–430
12. Ablasser, A., Goldeck, M., Cavlar, T., Deimling, T., Witte, G., Röhl, I., Hopfner, K. P., Ludwig, J., and Hornung, V. (2013) cGAS produces a 2′-5′-linked cyclic dinucleotide second messenger that activates STING. *Nature* **498,** 380–384
13. Diner, E. J., Burdette, D. L., Wilson, S. C., Monroe, K. M., Kellenberger, C. A., Hyodo, M., Hayakawa, Y., Hammond, M. C., and Vance, R. E. (2013) The innate immune DNA sensor cGAS produces a noncanonical cyclic dinucleotide that activates human STING. *Cell Rep.* **3,** 1355–1361
14. Gao, P., Ascano, M., Wu, Y., Barchet, W., Gaffney, B. L., Zillinger, T., Serganov, A. A., Liu, Y., Jones, R. A., Hartmann, G., Tuschl, T., and Patel, D. J. (2013) Cyclic [G(2′,5′)pA(3′,5′)p] is the metazoan second messenger produced by DNA-activated cyclic GMP-AMP synthase. *Cell* **153,** 1094–1107
15. Civril, F., Deimling, T., de Oliveira Mann, C. C., Ablasser, A., Moldt, M., Witte, G., Hornung, V., and Hopfner, K. P. (2013) Structural mechanism of cytosolic DNA sensing by cGAS. *Nature* **498,** 332–337
16. Burdette, D. L., Monroe, K. M., Sotelo-Troha, K., Iwig, J. S., Eckert, B., Hyodo, M., Hayakawa, Y., and Vance, R. E. (2011) STING is a direct innate immune sensor of cyclic di-GMP. *Nature* **478,** 515–518
17. Zhang, X., Shi, H., Wu, J., Zhang, X., Sun, L., Chen, C., and Chen, Z. J. (2013) Cyclic GMP-AMP containing mixed phosphodiester linkages is an endogenous high-affinity ligand for STING. *Mol. Cell* **51,** 226–235
18. Jin, L., Hill, K. K., Filak, H., Mogan, J., Knowles, H., Zhang, B., Perraud, A. L., Cambier, J. C., and Lenz, L. L. (2011) MPYS is required for IFN response factor 3 activation and type I IFN production in the response of cultured phagocytes to bacterial second messengers cyclic-di-AMP and cyclic-di-GMP. *J. Immunol.* **187,** 2595–2601
19. Danilchanka, O., and Mekalanos, J. J. (2013) Cyclic dinucleotides and the innate immune response. *Cell* **154,** 962–970
20. Gao, P., Ascano, M., Zillinger, T., Wang, W., Dai, P., Serganov, A. A., Gaffney, B. L., Shuman, S., Jones, R. A., Deng, L., Hartmann, G., Barchet, W., Tuschl, T., and Patel, D. J. (2013) Structure-function analysis of STING activation by c[G(2′,5′)pA(3′,5′)p] and targeting by antiviral DMXAA. *Cell* **154,** 748–762
21. Huang, Y. H., Liu, X. Y., Du, X. X., Jiang, Z. F., and Su, X. D. (2012) The structural basis for the sensing and binding of cyclic di-GMP by STING. *Nat. Struct. Mol. Biol.* **19,** 728–730
22. Tanaka, Y., and Chen, Z. J. (2012) STING specifies IRF3 phosphorylation by TBK1 in the cytosolic DNA signaling pathway. *Sci. Signal.* **5,** ra20
23. Stetson, D. B., and Medzhitov, R. (2006) Recognition of cytosolic DNA activates an IRF3-dependent innate immune response. *Immunity* **24,** 93–103
24. Hiscott, J. (2007) Triggering the innate antiviral response through IRF-3 activation. *J. Biol. Chem.* **282,** 15325–15329
25. Kirshner, J. R., Karpova, A. Y., Kops, M., and Howley, P. M. (2005) Identification of TRAIL as an interferon regulatory factor 3 transcriptional target. *J. Virol.* **79,** 9320–9324
26. Goubau, D., Romieu-Mourez, R., Solis, M., Hernandez, E., Mesplède, T., Lin, R., Leaman, D., and Hiscott, J. (2009) Transcriptional re-programming of primary macrophages reveals distinct apoptotic and anti-tumoral functions of IRF-3 and IRF-7. *Eur. J. Immunol.* **39,** 527–540
27. Bijl, M., and Kallenberg, C. G. (2006) Ultraviolet light and cutaneous lupus. *Lupus* **15,** 724–727
28. Caricchio, R., McPhie, L., and Cohen, P. L. (2003) Ultraviolet B radiation-induced cell death: critical role of ultraviolet dose in inflammation and lupus autoantigen redistribution. *J. Immunol.* **171,** 5778–5786
29. Yu, C., Chang, C., and Zhang, J. (2013) Immunologic and genetic considerations of cutaneous lupus erythematosus: a comprehensive review. *J. Autoimmun.* **41,** 34–45
30. Gehrke, N., Mertens, C., Zillinger, T., Wenzel, J., Bald, T., Zahn, S., Tüting, T., Hartmann, G., and Barchet, W. (2013) Oxidative damage of DNA confers resistance to cytosolic nuclease TREX1 degradation and potentiates STING-dependent immune sensing. *Immunity* **39,** 482–495
31. Kuhn, A., Herrmann, M., Kleber, S., Beckmann-Welle, M., Fehsel, K., Martin-Villalba, A., Lehmann, P., Ruzicka, T., Krammer, P. H., and Kolb-Bachofen, V. (2006) Accumulation of apoptotic cells in the epidermis of patients with cutaneous lupus erythematosus after ultraviolet irradiation. *Arthritis Rheum.* **54,** 939–950
32. Konno, H., Konno, K., and Barber, G. N. (2013) Cyclic dinucleotides trigger ULK1 (ATG1) phosphorylation of STING to prevent sustained innate immune signaling. *Cell* **155,** 688–698
33. Kemp, M. G., Gaddameedhi, S., Choi, J. H., Hu, J., and Sancar, A. (2014) DNA repair synthesis and ligation affect the processing of excised oligonucleotides generated by human nucleotide excision repair. *J. Biol. Chem.* **289,** 26574–26583
34. Iwamura, T., Yoneyama, M., Yamaguchi, K., Suhara, W., Mori, W., Shiota, K., Okabe, Y., Namiki, H., and Fujita, T. (2001) Induction of IRF-3/-7 kinase and NF-κB in response to double-stranded RNA and virus infection: common and unique pathways. *Genes Cells* **6,** 375–388
35. Yang, X., Boehm, J. S., Yang, X., Salehi-Ashtiani, K., Hao, T., Shen, Y., Lubonja, R., Thomas, S. R., Alkan, O., Bhimdi, T., Green, T. M., Johannessen, C. M., Silver, S. J., Nguyen, C., Murray, R. R., Hieronymus, H., Balcha, D., Fan, C., Lin, C., Ghamsari, L., Vidal, M., Hahn, W. C., Hill, D. E., and

Root, D. E. (2011) A public genome-scale lentiviral expression library of human ORFs. *Nat. Methods* **8,** 659–661
36. Hirt, B. (1967) Selective extraction of polyoma DNA from infected mouse cell cultures. *J. Mol. Biol.* **26,** 365–369
37. Hu, J., Choi, J. H., Gaddameedhi, S., Kemp, M. G., Reardon, J. T., and Sancar, A. (2013) Nucleotide excision repair in human cells: fate of the excised oligonucleotide carrying DNA damage *in vivo*. *J. Biol. Chem.* **288,** 20918–20926
38. Choi, J. H., Gaddameedhi, S., Kim, S. Y., Hu, J., Kemp, M. G., and Sancar, A. (2014) Highly specific and sensitive method for measuring nucleotide excision repair kinetics of ultraviolet photoproducts in human cells. *Nucleic Acids Res.* **42,** e29
39. Nelson, P., Rylance, P., Roden, D., Trela, M., and Tugnet, N. (2014) Viruses as potential pathogenic agents in systemic lupus erythematosus. *Lupus* **23,** 596–605
40. Zandman-Goddard, G., and Shoenfeld, Y. (2003) SLE and infections. *Clin. Rev. Allergy Immunol.* **25,** 29–40
41. Sancar, A. (1996) DNA excision repair. *Annu. Rev. Biochem.* **65,** 43–81
42. Wood, R. D. (1997) Nucleotide excision repair in mammalian cells. *J. Biol. Chem.* **272,** 23465–23468
43. Reardon, J. T., and Sancar, A. (2005) Nucleotide excision repair. *Prog. Nucleic Acid Res. Mol. Biol.* **79,** 183–235
44. Sancar, A., Lindsey-Boltz, L. A., Unsal-Kaçmaz, K., and Linn, S. (2004) Molecular mechanisms of mammalian DNA repair and the DNA damage checkpoints. *Annu. Rev. Biochem.* **73,** 39–85
45. Hildesheim, J., and Fornace, A. J., Jr (2004) The dark side of light: the damaging effects of UV rays and the protective efforts of MAP kinase signaling in the epidermis. *DNA Repair* **3,** 567–580
46. Schaap, P. (2013) Cyclic di-nucleotide signaling enters the eukaryote domain. *IUBMB Life* **65,** 897–903
47. Seth, R. B., Sun, L., Ea, C. K., and Chen, Z. J. (2005) Identification and characterization of MAVS, a mitochondrial antiviral signaling protein that activates NF-κB and IRF 3. *Cell* **122,** 669–682
48. Nazio, F., Strappazzon, F., Antonioli, M., Bielli, P., Cianfanelli, V., Bordi, M., Gretzmeier, C., Dengjel, J., Piacentini, M., Fimia, G. M., and Cecconi, F. (2013) mTOR inhibits autophagy by controlling ULK1 ubiquitylation, self-association and function through AMBRA1 and TRAF6. *Nat. Cell Biol.* **15,** 406–416
49. Corazzari, M., Fimia, G. M., and Piacentini, M. (2012) Dismantling the autophagic arsenal when it is time to die: concerted AMBRA1 degradation by caspases and calpains. *Autophagy* **8,** 1255–1257
50. Fimia, G. M., Corazzari, M., Antonioli, M., and Piacentini, M. (2013) Ambra1 at the crossroad between autophagy and cell death. *Oncogene* **32,** 3311–3318
51. Pagliarini, V., Wirawan, E., Romagnoli, A., Ciccosanti, F., Lisi, G., Lippens, S., Cecconi, F., Fimia, G. M., Vandenabeele, P., Corazzari, M., and Piacentini, M. (2012) Proteolysis of Ambra1 during apoptosis has a role in the inhibition of the autophagic pro-survival response. *Cell Death Differ.* **19,** 1495–1504
52. Schmidt, E., Tony, H. P., Bröcker, E. B., and Kneitz, C. (2007) Sun-induced life-threatening lupus nephritis. *Ann. N.Y. Acad. Sci.* **1108,** 35–40
53. Stern, R. S., and Docken, W. (1986) An exacerbation of SLE after visiting a tanning salon. *JAMA* **255,** 3120